(151) The LGLE-H design allows to easily insert, if desired, an optical flat, or curved, or segmented, etc. band pass filter 180 between the reflectors 148 and 152 to spectrally filter the concentration beam at a location where the intensity at the filter surface is low, thereby reducing filter deterioration through long term light exposure and overheating. This design feature is useful for high power MLE system where a spectral filter 180 cannot be located near the respective MES 144, without degrading the filter over time in an unacceptable manner. Optionally such a filter element can be rotated continuously or semi-continuously to minimize local filter overheating. If need, a variable beam attenuator can also be positioned conveniently near the location of the filter 180 shown in FIG. 13. Alternatively, such an attenuator can be placed in front of the input port of the respective LG 186.

(152) Asymmetric beam reformatting of the concentrated energy at the MES 144 can be accomplished, as discussed above with one or more respective ABT's. For example, FIG. 13 shows the case where an ABT 184 connects to a constant cross sectional shaped LG 186 that has a biased exit surface as an special output port configuration that is tilted against the beams z-axis (=auxiliary prism) thus providing an additional beam steering function. The type of ABT shown here is a hollow or solid LG 184 that is either a separate part that is attached to the input port of the LG 186 or is a special input surface preparation of the respective input port. For example, FIG. 13 shows the example of a CPC as a preferred cross sectional shape in the vertical plane, that is used to lower the vertical divergence angle from .theta..sub.v to .theta..sup.e.sub.v, and is an ABT that changes the direction of each ray with substantially only a single reflection interaction. In order to change the respective divergence in two directions, a bi-axial CPC shape can be used. Typically such asymmetric CPC-type shaped anamorphic beam transforming, light guiding, reflective hollow, or total internal reflecting solid elements, have the highest etendue efficiency for a given angular conversion task since only one reflection interaction is by design used to modify the beam directional angle with respect to its optical axis. This makes them very space and high throughput efficient. Depending on the desired beam reformatting task in a given preference plane (reducing or increasing the respective divergence angles). Other types of non-imaging, etendue or quasi etendue efficient shapes can be chosen. For example: a trumpet shape, a conical shape, a section of an oboloid or ellipsoid, a hyperbolical shape, i.e many other types of shapes as discussed for example in the book High Collection Non Imaging Optics by Welford and Winston). Due to this minimal interaction between such a type of ABT and the incoming beam they are typically not also able to spatially homogenize a beam so that SBT need to be used as beam homigenizer. For example, FIG. 13 shows the use of a constant cross sectional, rectangular integrator rod, i.e. LG 186.

(153) Alternatively the LG 186 can just be a conventional, constant cross sectional shape, LG that is used for energy collection and remote delivery as discussed above to form a respective LGLE-H.

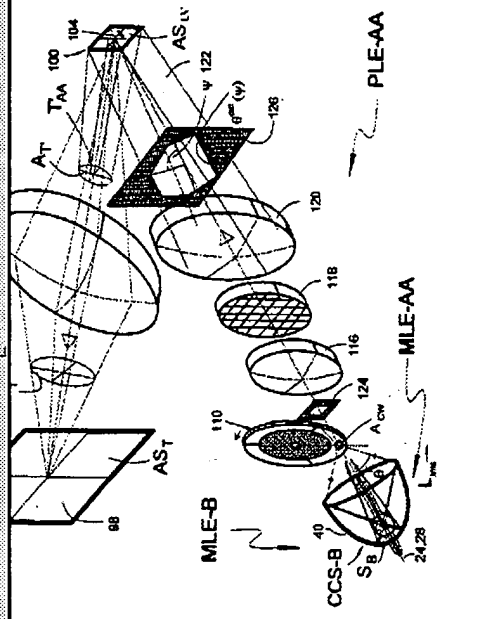

across the electrode sets, domain reversal occurs in regions o high voltage pulses. The range of the applied electric field several kV per cm to several 100 kV per cm. Domain reversal o entire crystal wafer so that substantially straight, vertical in the z plane are obtained so that the full crystal volume ca nonlinear interaction. The patterned high voltage field is ap temperature across the crystal. The processing of E-field pol in the articles of Jonas Webjorn et al., Quasi-Phase-Matched B Generation in Bulk Lithium Niobate, Electrically Poled via Per Electrodes, Electronic Letters, Vol. 30(11), pp. 894-895, May "Electric Field Induced Periodic Domain Inversion in Nd.sup.3+ LiNbO.sub.3 ", Electronic Letters, Vol. 30(25), pp. 2135-2136 and L. E. Myers et al., Quasi-Phase-Matched 1.064-.mu.m-Pumped Parametric Oscillator in Bulk Periodically Poled LiNbO.sub.3 " Vol. 20(1), pp. 52-54 (Jan. 1, 1995), which are incorporated reference thereto.

(29) A DFM rare earth doped, periodic poled nonlinear crysta functioning as rare earth doped oscillator may be employed usi architecture of device 35. In this case, a single laser diode provides wavelength, .lambda..sub.1, and device 35 would be a nonlinear material, such as LiNbO.sub.3 or KTP doped with Er.s Yb.sup.3+, Pr.sup.3+, or Tm.sup.3+, and is periodically poled, annealed proton exchange, titanium diffusion or E-field poling doped oscillator 35 is provided with reflectors 36A and 36B at output surfaces or may have reflectors positioned in an extern forming an external resonator. The input pump beam is partial longer wavelength by pumping the rare earth doped oscillator. pump radiation wavelength within the rare earth doped oscillat difference frequency mixes within the crystal with the interna longer radiation wavelength to generate even longer radiation generated longer wavelength is internally reflected within the the reflector coatings, which are chosen to provide high refle longer wavelengths. The periodic poling period is chosen so a match the DFM interaction. Examples of representative wavelen for mid-IR wavelengths, for example, useful in spectroscopy ar 1 below.

(1) TABLE 1 Rare Earth Doped Pumping Wave- Lithium Niobate Wavelength Dopant length, .lambda..sub.1, Range Lasing Wavele Nd.sup.3+ 805 m-810 nm 1060 nm 3.3 .mu.m-3.4 .mu.m Yb.sup.3+ 1120 nm-1150 nm 4.3 .mu.m-5.2 .mu.m Tm.sup.3+ 1120 nm-1200 nm .mu.m-4.8 .mu.m Er.sup.3+ 980 nm 1520 nm-1580 nm 2.6 .mu.m-2. Pr.sup.3+ 1010 nm-1020 nm 1290 nm-1330 nm 4.2 .mu.m-4.4 .mu.m

(30) Reference is now made to the embodiment shown in FIG. 1 pumped mid-IR wavelength source 50, which is an example of the

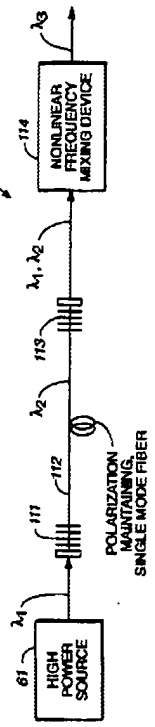

FIG._19

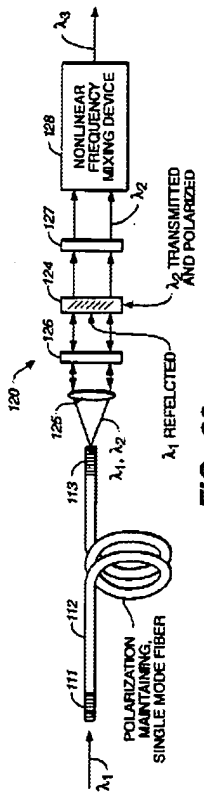

FIG._20

US-PAT-NO: 6229828

DOCUMENT-IDENTIFIER: US 6229828 B1

TITLE: High power pumped MID-IR wavelength devi
nonlinear frequency mixing (NFM)

DATE-ISSUED: May 8, 2001

INVENTOR-INFORMATION:

NAME	CITY	STATE
Sanders; Steven	Mountain View	CA
Lang; Robert J.	Pleasanton	CA
Waarts; Robert G.	Fremont	CA

ASSIGNEE INFORMATION:

NAME	CITY	STATE	Z
SDL, Inc.	San Jose	CA	N

APPL-NO: 09/ 123387

DATE FILED: July 27, 1998

PARENT-CASE:

CROSS REFERENCE TO RELATED APPLICATION

This application is a divisional application of application 08/649,560, filed May 17, 1996 now U.S. Pat. No. 5,912,910, incorporated herein by its reference.

INT-CL: [07] H01S003/10

US-CL-ISSUED: 372/22, 372/20 , 372/34 , 372/37 , 372/70 , , 372/102 , 359/326

US-CL-CURRENT: 372/22, 359/326 , 372/102 , 372/20 , 372/34 , 372/70 , 372/75

FIELD-OF-SEARCH: 372/20; 372/22 ; 372/6 ; 372/70 ; 372/75 ; 3 ; 372/102 ; 359/326

REF-CITED:

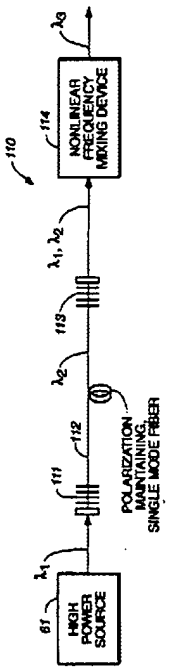

FIG._19

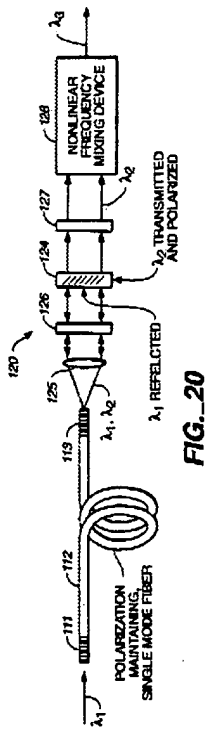

FIG._20

elliptically polarized eigenmodes for the propagation of light beams in acousto-optical modulator cell 47 comprising an optically active anisotropic crystal. The elliptical polarization of the eigenmodes of acousto-optical modulator cell 47 and the boundary conditions that must be satisfied by electric and magnetic fields of light beams being reflected and refracted at interfaces of optically active anisotropic crystals generate the first subset of the secondary output beams. , These certain of the secondary output beams generally have reduced intensities in the apparatus of the first embodiment. The first subset of the secondary beams have directions of propagation different from the directions of propagation of output beams 30 and 31 principally because of properties of birefringent truncated prisms 70 and 80.

(8) Input beam 18 enters acousto-optical modulator cell 47 and, through an acousto-optical interaction with a first acoustic beam, is converted to an intermediate beam. The intensity of the intermediate beam is preferably substantially the same as the intensity of input beam 18. The intermediate beam subsequently passes through a second acoustic beam. By way of an acousto-optical interaction of the intermediate beam with the second acoustic beam, a portion of the intermediate beam is converted into a beam exiting acousto-optical apparatus 40 as one of the output beams 30 and 31 with the remaining non-converted portion of the intermediate beam exiting acousto-optical apparatus 40 as the other of the output beams 30 and 31.

(9) Incomplete conversion of input beam 18 into the intermediate beam generates a second subset of the secondary output beams. The second subset o the secondary beams have reduced intensities in the apparatus of the first embodiment and have directions of propagation different from the directions o propagation of output beams 30 and 31.

(10) Acousto-optical interaction of acoustic beams that result from a porti of the second acoustic beam reflected by absorber 68 and the optical beam remaining as a result of incomplete conversion of input beam 18 into the intermediate beam may generate a third set of beams of the secondary beams. The third set of secondary beams have in the apparatus of the first embodimen reduced intensities, frequencies different from the frequencies of output bea 30 and 31. However, the direction of propagation of the third set of seconda beams is parallel to the directions of propagation of output beams 30 and 31.

(11) Eigenmodes for propagation of light beams in optically active anisotropic crystals generally comprise two modes, a left-handed rotating elliptically polarized mode and a right-handed rotating elliptically polarize mode. The two eigenmodes for light beam propagation in a left-handed rotatin positive uniaxial crystal are left-handed and right-handed rotating elliptically polarized modes with the major axes of the eigenmodes coinciding with the directions of polarization of ordinary and extraordinary polarized beams, respectively. The major axes of a left-handed rotating elliptically polarized beam and a right-handed rotating elliptically polarized beam are

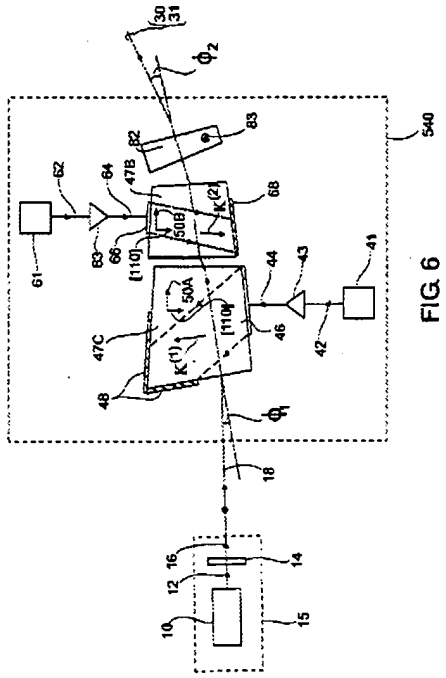

FIG 6

US-PAT-NO: 5657152

DOCUMENT-IDENTIFIER: US 5657152 A

TITLE: Acoustooptic device

DATE-ISSUED: August 12, 1997

INVENTOR-INFORMATION:

NAME	CITY	STATE	ZIP CODE	
Kadota; Michio	Kyoto	N/A	N/A	

ASSIGNEE INFORMATION:

NAME	CITY	STATE	ZIP CODE	COUNTR
Murata Manufacturing Co., Ltd.	N/A	N/A	N/A	JP

APPL-NO: 08/ 616528

DATE FILED: March 19, 1996

FOREIGN-APPL-PRIORITY-DATA:

COUNTRY	APPL-NO	APPL-DATE
JP	7-091681	March 24, 1995

INT-CL: [06] G02F001/33,G02F001/035

US-CL-ISSUED: 359/305, 359/285 , 385/2 , 385/7 , 310/313D , 310/313B

US-CL-CURRENT: 359/305, 310/313B , 310/313D , 359/285 , 385/2 , 385/7

FIELD-OF-SEARCH: 359/305; 359/285 ; 385/2 ; 385/7 ; 385/1 ; 310/313D ; 310/313B

REF-CITED:

U.S. PATENT DOCUMENTS

PAT-NO	ISSUE-DATE	PATENTEE-NAME		
4127320	November 1978	Li	N/A	N/A
4418980	December 1983	Keil et al.	N/A	N/A
4544229	October 1985	Verber		

FIG. 7 PRIOR ART

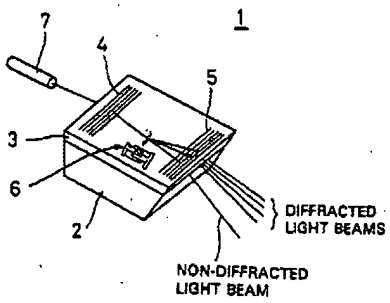

FIG. 8 PRIOR ART

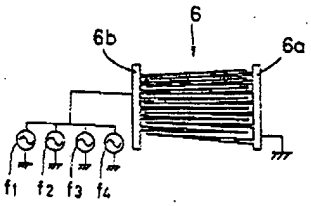

(2) 1. Field of the Invention

(3) The present invention relates to an acoustooptic device, and particularl to an acoustooptic device which is preferably used as a light deflecting devic for a laser printer or other suitable device.

(4) 2. Description of the Related Art

(5) FIG. 7 is a perspective view showing a conventional acoustooptic device, and FIG. 8 is a diagram showing a main part of the acoustooptic device of FIG. 7. The acoustooptic device deflects light beams by using an interaction between light and ultrasonic waves such as surface acoustic waves. The acoustooptic device 1 includes a LiNbO.sub.3 layer 2 of Y-cut, and an optical waveguide layer 3 which is formed of a thin film of Nb.sub.2 O.sub.5 is locate on the LiNbO.sub.3 layer 2. An input grating 4 is located on the principal plane at a light input side of the optical waveguide layer 3 so as to be substantially perpendicular to a light incident direction. An output grating is located on the principal plane at a light output side of the optical waveguide layer 3 so as to be substantially parallel to the input grating 4. The input grating 4 and the output grating 5 collect spatial light beams into the optical waveguide and combine the spatial light beams. The input grating and the output grating 5 are formed as plural grooves which are parallel to on another, or formed of plural rod-shaped electrodes which are parallel to one another.

(6) Further, an interdigital electrode 6 is located on the principal plane o the optical waveguide layer 3 so that a Rayleigh wave, which is a kind of surface acoustic wave, is excited at the intermediate portion between the inpu grating 4 and the output grating 5. The interdigital electrode 6 is formed of a pair of comb-shaped electrodes 6a and 6b which are mutually inserted into each other (or interdigitated) as shown in FIG. 8. One comb-shaped electrode 6a is grounded while the other comb-shaped electrode 6b is connected to an oscillator for applying a frequency.

(7) In the acoustooptic device 1, a Rayleigh wave is excited so as to have a frequency corresponding to a frequency applied by the interdigital electrode 6 One light beam is incident from a light source 7 into the optical waveguide layer 3 of the acoustooptic device 1. The light beam which is incident from the light source 7 into the optical waveguide layer 3 is diffracted by the Rayleigh wave which is excited by the applied frequency, so that a different light diffraction (deflection) angle can be obtained by changing the frequency applied to the interdigital electrode 6. The acoustooptic device 1 may be use as a light deflection device for a laser printer or the like.

(8) The variation (variable width) .DELTA..theta. of a light deflection angle at which the light beam is diffracted in accordance with the variation .DELTA.f of the frequency is represented by the following equation:

FIG. 7 PRIOR ART

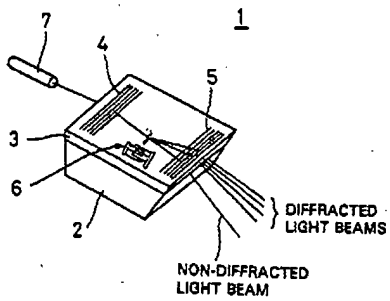

FIG. 8 PRIOR ART

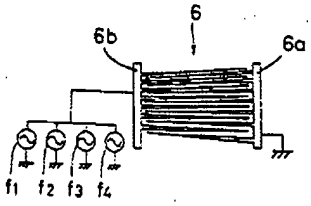

rotation constant in units of degrees per centimeter, and k.sub.opt is the magnitude of the optical wavevector.

(22) In general, the component of the RF magnetization along the direction o optical propagation results in a traveling refractive index grating which can diffract between orthogonally polarized optical modes. For example, the .epsilon..sub.13 and .epsilon..sub.31 optical permittivity elements of Equatio (10) will induce coupling between the TE and TM waveguide modes of an optical wave with a component of travel (k.sub.opt) along the Y axis direction in the configuration of FIG. 3. Thus, due to the interaction between the TM input guided optical wave and the MSW, a portion of the TM mode wave is coupled into the orthogonal TE mode while the remaining portion of the guided optical wave remains in the TM mode. The amplitude of the guided optical beam coupled into the TE mode is proportional to the input signal 30 which excites the MSW. Thu the guided optical wave is modulated by the MSW. The optical frequency .omega..sub.d of the diffracted beam is doppler shifted by the MSW to .omega..sub.d =.omega.+.OMEGA. when k.sub.d =k.sub.i +k.sub.m holds or .omega .sub.d =.omega.-.OMEGA. when k.sub.d =k.sub.i -k.sub.m.

(23) The growth of the converted mode intensity I.sub.d with distance y follows from coupled mode theory as ##EQU4##

(24) In each of the devices 10 and 100 illustrated respectively in FIGS. 1 and 3, a TM polarization mode optical input beam has been converted to an orthogonal TE mode output beam due to the interaction with the MSW in the thin film layer. Alternatively, a TE mode laser beam can be used as an input. In this case, the modulated output beam will be in the orthogonal TM mode. The spatial positions of the input and output beams with regard to the input and output prisms will, of course, change depending on the polarization modes of the various beams.

(25) In the devices 10 and 100 shown respectively in FIGS. 1 and 3, a ground plane for the stripline antenna has been formed by depositing a metallic layer 20 on the lower planar surface 18 of the substrate 12. Alternatively, a groun plane could be formed by depositing a metallic layer on the upper planar surface of an alumina plate (not illustrated) of several mils thickness. The uncoated lower surface of the alumina plate could than be positioned above the upper planar surface 28 of the thin film layer 14 such that the antenna metallization and the magnetic absorber layer are sandwiched between the alumina plate and the thin film layer and are in contact with the plate. In this alternative configuration, the thickness of the alumina plate could be adjusted to optimize the ground plane effect. It should be appreciated that appropriate openings must be formed in the alumina plate to provide clearance for the two prisms which contact the upper surface 28 of the thin film layer. As yet another alternative, the antenna metalization and the magnetic absorber layer could be deposited on the lower surface of the alumina plate with the upper surface of the plate being coated with the ground plane metalization.

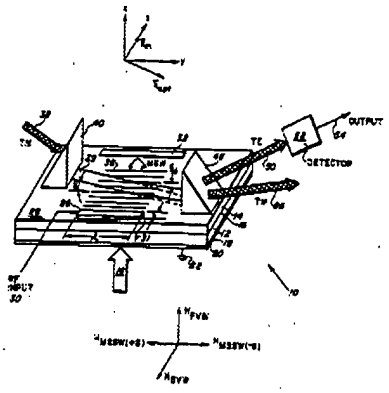

FIG. 1

to N-1 during the integration time T. Equation 8 can be evaluated, yielding ##EQU9## Noting that Ne.sub..omega. =.DELTA..omega., the total hopper bandwidth, yields ##EQU10##

(14) The Two-Dimensional Frequency Scanning Correlator of the Invention

(15) As mentioned above, the useful integration time of the two beam correlator that has been described above is limited when it is used as a cross-correlation signal detector by any difference between the reference carrier frequency and the input signal carrier frequency. This limit can be estimated by examining the correlator response to two single-frequency cw signals, cos .omega..sub.A t and cos .omega..sub.B t. From equation 5 one obtains ##EQU11## When the frequency difference, .omega..sub.B -.omega..sub.A is equal to 2.pi./T, the output goes to zero because of the sinc term. For a 30-ms integration time, this corresponds to about a 200-Hz frequency difference.

(16) A proposed scheme for avoiding this problem, and at the same time determining the frequency offset between the reference and the input signal, illustrated in FIG. 5. The reference signal, A(t) cos .omega..sub.A t, is input to a surface acoustic wave delay line 20 which is illuminated by a shee beam of laser light. The signal to be detected, B(t) cos .omega..sub.B t is input to a second surface acoustic wave delay line 22 which is illuminated by sheet beam of light derived from the same laser 24. The laser beam is split a beam splitter (26), and the respective resulting beams are phase equalized E-O phase modulator 28, and are fed through beam expanders 30 and 32, and cylindrical lenses 34 and 36. The diffracted beams from the two delay lines can be described as ##EQU12## This light is compressed (focussed) in the X dimension by lenses 38 and 40, and expanded in the Y dimension by lenses 42 a 44, and is used to illuminate a third delay line 46. Thus, first, second, third and fourth beams, 50, 52, 54 and 56 are incident on the acousto-optic interaction means. The geometry is such that this third delay line 46 operat in the same manner as the one-dimensional time integrating correlator previously described. The inputs to this third delay line are identical chirps, cos (.omega..sub.c +.alpha.t)t, and the light diffracted by the counter-propagating surface acoustic waves generated by the chirps is expande in the X dimension: This light can be described by ##EQU13## The two-dimensional detector diode array squares the sum of these two light beams and the array output contains a term ##EQU14## Proper choice of the chirp rat .alpha. will guarantee that at some Y value (Y.sub.o) the time variable part of the cosine time, [.omega..sub.B -.omega..sub.A -4.alpha.Y/v.sub.a]t, will vanish, yielding ##EQU15## Thus, the cross-correlation of A(t) and B(t) is obtained in spite of the difference in carrier frequencies. In the Y dimensi the output is the autocorrelation of the chirp cos (.omega..sub.c +.alpha.t)t Hence, the frequency offset between .omega..sub.A and .omega..sub.B can be determined from the location of the correlation peak in the Y coordinate.

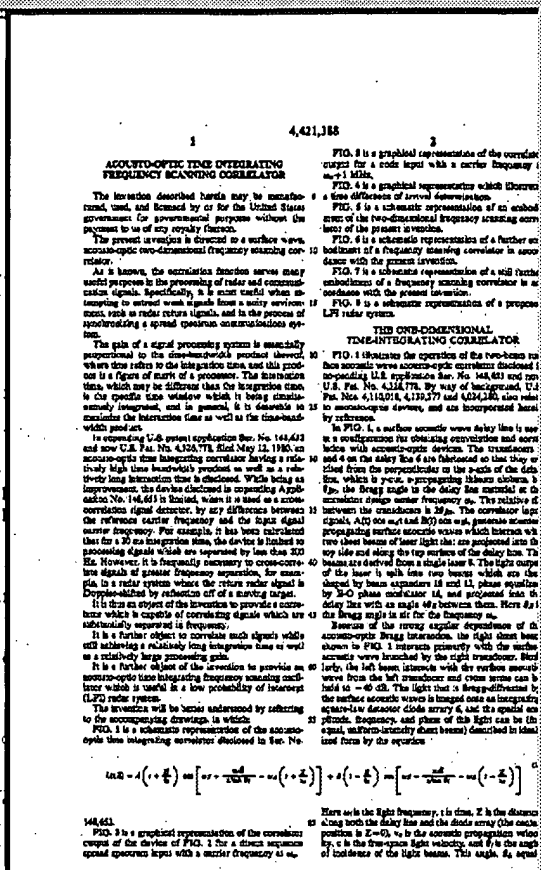

4,421,388

1

ACOUSTO-OPTIC TIME INTEGRATING FREQUENCY SCANNING CORRELATOR

The invention described herein may be manufactured, used, and licensed by or for the United States government for governmental purposes without the payment to us of any royalty thereon.

The present invention is directed to a surface wave, acousto-optic two-dimensional frequency scanning correlator.

As is known, the correlation function serves many useful purposes in the processing of radar and communication signals. Specifically, it is most useful when attempting to extract weak signals from a noisy environment, such as radar return signals, and in the process of synchronizing a spread spectrum communications system.

The gain of a signal processing system is essentially proportional to the time-bandwidth product thereof, where time refers to the integration time and this product is a figure of merit of a processor. The interaction time, which may be different than the integration time, is the specific time window which is being simultaneously integrated, and in general, it is desirable to maximize the interaction time as well as the time-bandwidth product.

In copending U.S. patent application Ser. No. 144,633 and now U.S. Pat. No. 4,326,778, filed May 12, 1980, an acousto-optic time integrating correlator having a relatively high time bandwidth product, as well as a relatively long interaction time is disclosed. While being an improvement, the device disclosed in copending Application No. 144,633 is limited, when it is used as a cross-correlation signal detector, by any difference between the reference carrier frequency and the input signal carrier frequency. For example, it has been calculated that for a 30 ms integration time, the device is limited to processing signals which are separated by less than 300 Hz. However, it is frequently necessary to cross-correlate signals of greater frequency separation, for example in a radar system where the return radar signal is Doppler-shifted by reflection off of a moving target.

It is thus an object of the invention to provide a correlator which is capable of correlating signals which are substantially separated in frequency.

It is a further object to correlate such signals while still achieving a relatively long integration time as well as a relatively large processing gain.

It is a further object of the invention to provide an acousto-optic time integrating frequency scanning correlator which is useful in a low probability of intercept (LPI) radar system.

The invention will be better understood by referring to the accompanying drawings, in which:

FIG. 1 is a schematic representation of the acousto-optic time integrating correlator disclosed in Ser. No. 144,633.

FIG. 2 is a graphical representation of the correlator output for a code input with a carrier frequency of ω_0=1 MHz.

FIG. 3 is a graphical representation of the correlator output of the device of FIG. 1 for a chirp sequence spread spectrum input with a carrier frequency of ω_0.

2

FIG. 4 is a graphical representation which illustrates a time difference of arrival determination.

FIG. 5 is a schematic representation of an embodiment of the two-dimensional frequency scanning correlator of the present invention.

FIG. 6 is a schematic representation of a further embodiment of a frequency scanning correlator in accordance with the present invention.

FIG. 7 is a schematic representation of a still further embodiment of a frequency scanning correlator in accordance with the present invention.

FIG. 8 is a schematic representation of a proposed LPI radar system.

TWO DIMENSIONAL TIME-INTEGRATING CORRELATOR

FIG. 1 illustrates the operation of the two-beam surface acoustic wave acousto-optic correlator disclosed in copending U.S. application Ser. No. 144,633 and now U.S. Pat. No. 4,326,778. By way of background, U.S. Pat. Nos. 4,110,018, 4,139,277 and 4,224,180, also relate to acousto-optic devices, and are incorporated herein by reference.

In FIG. 1, a surface acoustic wave delay line is used in a configuration for obtaining convolution and correlation with acousto-optic devices. The transducers 4 and 6 on the delay line 8 are fabricated so that they are tilted from the perpendicular to the y-axis of the delay line, which is y-cut, x-propagating lithium niobate. In this, the Bragg angle in the delay line material at the correlator design center frequency ω_0. The relative tilt between the transducers is 2θ_B. The correlator input signals, A(t) cos ω_0t and B(t) cos ω_0t, generate acoustic propagating surface acoustic waves which interact with two short beams of laser light that are positioned into the way like and along the top surface of the delay line. The beams are derived from a single laser 9. The light output of the laser is split into two beams which are then changed by beam expanders 10 and 11, phase equalized by E-O phase modulator 12, and projected into the delay line with an angle 4θ_B between them. Here θ_B is the Bragg angle in air for the frequency ω_0.

Because of the strong angular dependence of the acousto-optic Bragg interaction, the light beam being shown in FIG. 1 interacts primarily with the surface acoustic wave launched by the right transducer. Similarly, the left beam interacts with the surface acoustic wave from the left transducer and cross terms can be held to −40 db. The light that is Bragg-diffracted by the surface acoustic waves is imaged onto an integrating square-law detector diode array 6, and the spatial separation, frequency, and phase of the light can be (the equal, uniform-intensity short beams) described in ideal time form by the equation

$$\text{[illegible]} = A\left(t+\frac{x}{v}\right)\cos\left[\omega_0 t - \frac{\omega_0}{2\sin\theta_B}\sin\left(\theta+\frac{x}{v}\right)\right] + A\left(t-\frac{x}{v}\right)\cos\left[\omega_0 t - \frac{\omega_0}{2\sin\theta_B}\sin\left(\theta-\frac{x}{v}\right)\right]$$

Here ω_0 is the light frequency, t is time, Z is the distance along both the delay line and the diode array (the coordinate position is Z=0), v_a is the acoustic propagation velocity, c is the free-space light velocity, and θ_i is the angle of incidence of the light beams. This angle, θ_B, equal

19, 2001, and U.S. Provisional Patent Application, Serial No. 60/277,480, entitled "LENS FOR AN OPTICAL SWITCH" filed Mar. 19, 2001, the contents of both of which are hereby incorporated by reference.

BRIEF SUMMARY:

FIELD OF THE INVENTION

[0002] The present invention is generally related to fiber optic switches and more particularly relates to multi-port, non-blocking optical switches.

BACKGROUND

[0003] Continuing innovations in the field of fiber optic technology have contributed to the increasing number of applications of optical fibers in various technologies. With the increased utilization of optical fibers, there is a need for efficient optical systems that assist in the transmission and the switching of optical signals. For example, there is presently a need for optical switches that direct the light signals from a set of input optical fibers to any of several output optical fibers, without converting the optical signal to an electrical signal. Light in this sense generally refers to the propagation of electromagnetic radiation and is not limited to the visible spectrum.

[0004] Various techniques may be utilized to couple optical fibers with a switch. For example, information may be digitally switched by converting the optical signal into a digital electrical signal, electrically routing the signal, and then regenerating an optical signal. This complex process offers the greatest traffic control but is very expensive and unnecessary for the majority of traffic passing through a switching node. Therefore, low-port-count MEMS-based optical switches are commonly used in communications systems to switch light from a plurality of input waveguides to a plurality of output waveguides without first converting the optical signal to an electrical signal. Such optical switches use MEMS mirrors as a reflective element, moving the mirror in or out of the path of a beam of light to redirect the optical signal path between stationary waveguides or collimating optics.

[0005] Many types of optical switches that utilize MEMS micro-mirrors have been proposed and tested. Two-dimensional arrays of bi-state micro-mirrors have been constructed that enable digital switching of optical signals. Monolithically interconnected arrays of 2.times.2 waveguide switches with thermal or electric field induced switching can provide the same function. This class of switches is commonly referred to as 2D due to their switching in a two-dimensional or planar surface. For a configuration with N inputs and N outputs, N.sup.2 switching nodes are required.

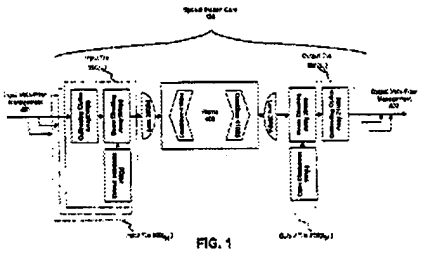

FIG. 1

BACKGROUND ART

[0003] Modern fiber optical communications systems direct optical signals over multiple fibers. Such systems require optical switches to direct light beams from any given fiber in an input fiber array to any given fiber in an output array. One class of optical switches uses an approach called beam steering. In beam steering, the light from the fiber is selectively deflected or steered by one or more movable optical element from the input fiber to the output fiber. Suitable optical elements include microelectromechanical system (MEMS) mirrors. MEMS mirrors are usually actuated by magnetic interaction, electrostatic, or piezoelectric interaction. Typically, two sets of moveable mirrors are used to steer the beam. Each fiber has a small "acceptance window". The fiber only efficiently couples light that is incident within a narrow range of angles and positions. Although a single mirror will generally direct the beam from an input fiber to the correct output fiber, two mirrors ensure that the light beam enters the output fiber at the correct angle. If the beam makes too large an angle with the axis of the fiber, light from the beam will not couple properly to the fiber, i.e. there will be high losses.

[0004] Optical switches using the steering-beam approach have been demonstrated in two primary implementations. The first uses linear arrays of mirrors with a single angular degree of freedom. Combining two such mirror arrays as shown in FIG. 1 allows an implementation of an N.times.N optical switch, where the number of input and output channels is equal to the number of mirrors in each array. The first array steers an optical beam from an input fiber to the appropriate mirror on the second array, which then steers the beam into the corresponding output fiber. This implementation uses simple single-axis mirrors; however, it is limited in its scalability since the optical path between fibers becomes unreasonably large for large port counts (e.g. >32.times.32), increasing the loss of the switch

[0005] The second implementation depicted in FIG. 2 uses two sets of 2-dimensional mirror arrays, each mirror having two angular degrees of freedom. The input and output fibers are each also arranged in a 2-dimensional grid with the same dimension as the mirror arrays. The mirrors in the first mirror array steer the optical beams from the fibers onto the appropriate mirror in the second mirror array which then steers the beam into the corresponding fiber. This approach is considerably more scalable, since, due to its 2-dimensional layout, the size of the mirror and fiber arrays grows as the square root of the number of input/output ports, which is much slower than in the case of a 1-dimensional grid. Therefore, switches with much larger port count (>2000.times.2000) are possible. However, this implementation requires the mirrors to rotate about two different axes. Such mirrors are considerably more difficult to design, fabricate, and control.

[0006] There is a need, therefore, for a beam steering apparatus that uses single axis optical elements to switch optical signals in an N.times.N fiber array

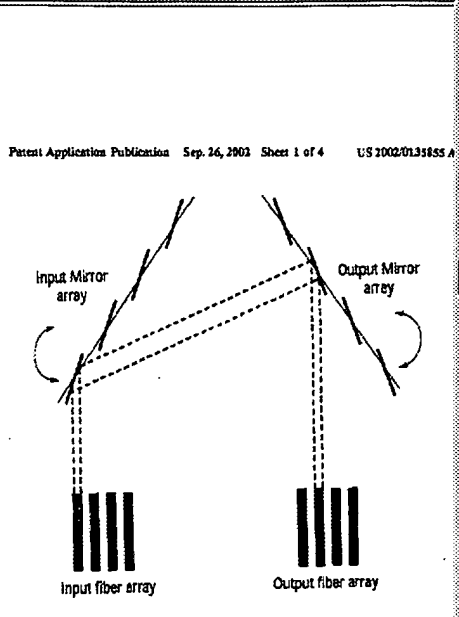

Fig. 1 (Prior Art)

4408a and output from the optical I/O port.

[0012] In FIG. 44(B), the optical deflector 4402 comprises the optical fiber 4408 inserted through the I/O port, a collimating lens 4410, a fixed mirror 4412, and a movable mirror 4414.

[0013] A light beam from the I/O port leaves from the end of the optical fiber 4408 that is housed in the optical deflector 4402. This light beam is focused or condensed by the collimating lens 4410 and reflected or deflected by the fixed mirror 4412 into the movable mirror 4414 at which it is reflected at a given deflection angle. The movable mirror 4414 has two rotation axes that are perpendicular to the incident direction of a light beam so as to be movable on two axes. The rotation of the movable mirror 4414 may be adjusted by an ordinary technique. Thus, the movable mirror 4414 is able to reflect the light beam to the mirror 4404 at a given deflection angle. The mirror 4404 then reflects the light beam toward the optical deflector 4402a.

[0014] The light beam put into the light deflector 4402a travels in the direction opposite to that of FIG. 44(B) and is deflected by the movable mirror 4414. Then, it is reflected by the fixed mirror 4412, condensed by the collimating lens 4410, and output from the I/O port via the optical fiber 4408a. The deflection angle is adjusted at the movable mirror 4414 to input the light beam into the optical fiber 4408a.

[0015] As has been described above, this optical switch is composed of one stage of optical deflectors using a movable mirror or lens to control the direction of a light beam into the predetermined I/O port. This optical switch employs 3-D wiring or interconnection so that it is easy to increase the number of ports.

[0016] However, the conventional optical switch requires very high precisions with which the light beam is deflected by a single deflector. Consequently, it has the following disadvantage.

[0017] The diameter of optical fibers for usual optical communication systems is approximately eight microns. If a light beam is input with a positional error of about one micron, a loss of one dB or more is generated, presenting a practical problem. The distance between the output ports required for mounting is a few 100 microns or more so that even a piece of two-channel equipment requires a precision of about 0.1% in deflection angle. If the equipment has tens of channels or more, the required precision is in the order of 10-4. The 100-channel equipment using movable mirrors requires a precision of about 1% in deflection angle. The equipment of 1000 channels or more requires a precision of 0.3%.

[0018] In order to solve the problem, it has been proposed to superimpose a position detecting signal on the light beam to detect the deflection angle and

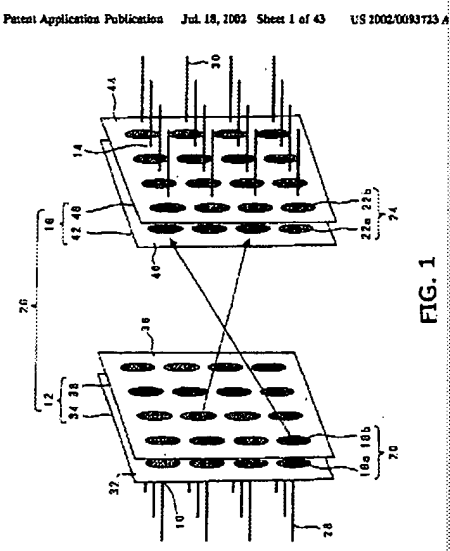

FIG. 1

BACKGROUND OF THE INVENTION

[0002] 1. Field of the Invention

[0003] The present invention relates generally to micro-electromechanical (MEMS) devices and, in particular, to arrayed magnetically actuated MEMS devices such as arrayed mirrors used in optical switches.

[0004] 2. Description of Related Art

[0005] FIG. 1 schematically illustrates an example of an optical cross-connect 12 of an optical switch. The cross-connect 12 includes an array of collimators or other beam-forming devices, represented by grid 14, and forms incoming optical communications signals into beams that impinge on an array of selectively moveable reflectors or mirrors represented by grid 16. Each beam from grid 14 has its own corresponding moveable mirror on grid 16.

[0006] The moveable mirrors of grid 16 are controllably positioned so as to individually direct the respective beams from grid 14 to respective moveable mirrors of a second array of moveable mirrors, represented by grid 18. The moveable mirrors of grid 18 are positioned so as to individually direct the beams received from grid 16 to respective beam receivers of an array of beam receivers represented by grid 20. The beam receivers may take various forms, such as transducers, lenses or optical elements for coupling the respective beams into respective optical fibers, waveguides, or the like. As with grids 14 and 16, each moveable mirror of grid 18 is associated with a particular beam receiver of grid 20, so that each receiver receives beams on a single axis. A representative signal path from grid 14 to grid 20 is indicated by arrow 22.

[0007] Attempts have been made previously to fabricate arrays of mirrors such as those represented by grids 16 and 18 using MEMS technology, in which silicon processing and related techniques common to the semiconductor industry are used to form micro-mechanical devices. For switches such as that shown in FIG. 1, it is desirable to have an array of moveable mirrors that are both densely packed and easily controlled.

[0008] As is known in the art, movable mirrors can be actuated or controlled in a variety of ways including through electromagnetic actuation, electrostatic actuation, piezoelectric actuation, stepper motors, thermal bimorph and comb-drive actuation.

[0009] FIG. 2 illustrates an electro-magnetically actuated single-mirror device 30 in accordance with the prior art. The mirror device 30 includes a mirror 32 movably supported on a gimbal structure 34. The mirror 32 includes a reflective surface 33, which is on the same side of the mirror as the actuation coils.

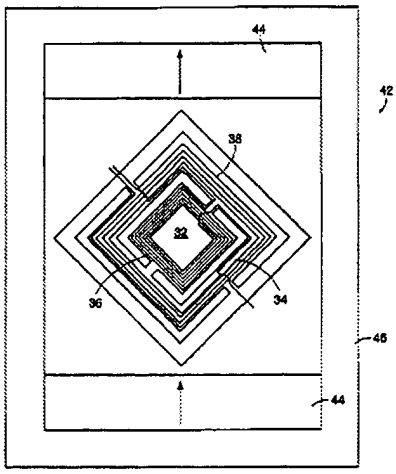

FIG. 3
PRIOR ART

~~29 Claims; 4 Drawing Figures~~

Exemplary Claim Number: 1

Number of Drawing Sheets: 4

BRIEF SUMMARY:

(1) FIELD OF THE INVENTION

(2) This invention relates generally to fiber optic communications. More particularly, the invention relates to optical switches for NxN arrays of fibers.

(3) BACKGROUND ART

(4) Modern fiber optical communications systems direct optical signals over multiple fibers. Such systems require optical switches to direct light beams from any given fiber in an input fiber array to any given fiber in an output array. One class of optical switches uses an approach called beam steering. In beam steering, the light from the fiber is selectively deflected or steered by one or more movable optical element from the input fiber to the output fiber. Suitable optical elements include microelectromechanical system (MEMS) mirrors. MEMS mirrors are usually actuated by magnetic interaction, electrostatic, or piezoelectric interaction. Typically, two sets of moveable mirrors are used to steer the beam. Each fiber has a small "acceptance window". The fiber only efficiently couples light that is incident within a narrow range of angles and positions. Although a single mirror will generally direct the beam from an input fiber to the correct output fiber, two mirrors ensure that the light beam enters the output fiber at the correct angle. If the beam makes too large an angle with the axis of the fiber, light from the beam will not couple properly to the fiber, i.e. there will be high losses.

(5) Optical switches using the steering-beam approach have been demonstrated in two primary implementations. The first uses linear arrays of mirrors with a single angular degree of freedom. Combining two such mirror arrays as shown in FIG. 1 allows an implementation of an NxN optical switch, where the number of input and output channels is equal to the number of mirrors in each array. The first array steers an optical beam from an input fiber to the appropriate mirror on the second array, which then steers the beam into the corresponding output fiber. This implementation uses simple single-axis mirrors; however, it is limited in its scalability since the optical path between fibers becomes unreasonably large for large port counts (e.g. >32.times.32), increasing the loss of the switch.

(6) The second implementation depicted in FIG. 2 uses two sets of 2-dimensional mirror arrays, each mirror having two angular degrees of freedom. The input and output fibers are each also arranged in a 2-dimensional grid with

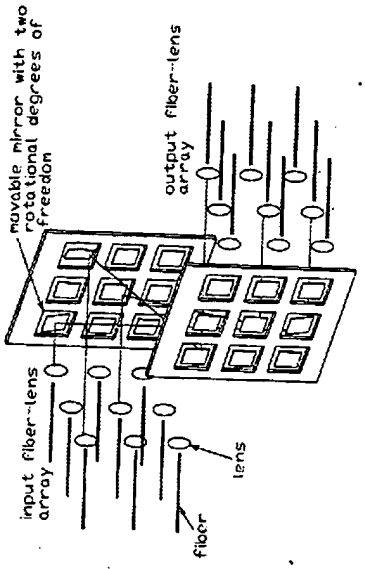

Fig.2